Jurnal Teknologi Reaktor Nuklir

Tri Dasa Mega

Journal homepage: jurnal.batan.go.id/index.php/tridm

Analysis of Thorium Pin Cell Burnup of the PWR using WIMS Code

Jonny Haratua Panggabean[1], Santo Paulus Rajagukguk*[1], Syaiful Bakhri[2]

[1)]Department of Physics, FMIPA, UNIMED, Medan, 20221, Indonesia
[2)]Research Center for Nuclear Reactor Technology, Research Organization for Nuclear Energy, BRIN, Kawasan Puspiptek Gd.80, Tangerang Selatan, 15314, Banten, Indonesia,

ARTICLE INFO

Article history:

Received: 23 May 2022
Received in revised form: 8 June 2022
Accepted: 14 June 2022

Keywords:

Thorium
PWR Fuel
Burn up
Pin Cell
WIMSD-5B

A B S T R A C T

A thorium-fueled benchmark comparison was made in this study between state-of-the-art codes, WIMSD-5B code to MOCUP (MCNP4B + ORIGEN2), and CASMO-4 for burnup calculations as an effort to examine the possible benefits of using thorium in PWR fuel. WIMSD-5B calculations employ the same model as a reference, while for MOCUP and CASMO, there are some differences in methodology and cross-section libraries. On a PWR pin cell model, eigenvalue and isotope concentrations were examined up to high burn-up. The eigenvalue comparison as a function of burn-up is in good agreement, with a maximum difference of less than 5% and an average absolute difference of less than 1%. The isotope concentration comparisons outperform a set of ThO_2-UO_2 fuel benchmarks and are comparable to a set of uranium fuel benchmarks previously published in the literature. As a burn-up function, the eigenvalue comparison is discussed in this paper. The actinide and fission product data sources for a typical thorium fuel are reported in the WIMSD-5B burnup calculations. The reasons for discrepancies in coding are examined and explored.

1. INTRODUCTION

The use of thorium fuel in pressurized water reactors (PWRs) has resurfaced due to its capacity to provide longer intra-refueling intervals and high burnup while lowering weaponizable material usefulness from spent fuel and boosting in-repository longevity. The use of thorium-based fuel in otherwise standard, retrofittable PWR fuel assemblies is the focus of this research. Between 1960 and 1980, thorium as a fuel for PWRs was actively investigated, including whole-core demonstrations at Indian Point I, Elk River, and the Shippingport Breeder [1]. Thorium utilization was also extensively investigated in the PRTRN-BRIN Indonesia programs, however, the focus was on recycling-mode fuel cycles with highly enriched U-235 for start-up and burnup of less than 30 MWd/kg [2].

However, circumstances have altered since then: once-through fueling is assumed, < 20% U-235 anti-proliferation limit has been enforced, and uranium-fueled PWRs have attained discharge burn-up approaching 60 MWd/kg [3], with more increases in the pipeline. Furthermore, a completely new generation of codes and cross-section sets is now available. As a result, we started a new set of computational benchmarks to represent these new realities. Using the WIMSD-5B code package and many libraries [4, 5], the zero leakage, poison-free pin cells were irradiated to over 70 MWd/kg at constant power. The calculated result will be compared to CASMO-4 and MOCUP [6]. Subject

*Corresponding author. Tel./Fax.:
E-mail: santopaulusrajagukguk98@gmail.com
DOI: 10.17146/tdm.2022.24.2.6626

programs are well-known and cutting-edge, also the difference between calculation and references will be discussed. The aim of this research is to understand the WIMSD-5B code capability in calculating the eigenvalues with different libraries.

2. BRIEF DESCRIPTION OF PWR CORE

Westinghouse designed the PWR and is well known in the world. Figure 1 shows the core configuration of a PWR reactor. At the start of the cycle (BOC), the PWR core is made up of three enrichment levels: 2.4 wt%, 3.1 wt%, and 3.9 wt% [7, 8]whose share are 49 fuel assemblies, 48 fuel assemblies, and 48 fuel assemblies, respectively [9]. In total, the PWR core is made up of 145 fuel assemblies. Table 1 summarizes the PWR pin cell parameter, fuel dimensions, and coolant parameter. A cylindrical fuel pellet with ThO_2-UO_2 is used in the PWR reactor, and the fuel cladding is Zircalloy-4 [10].

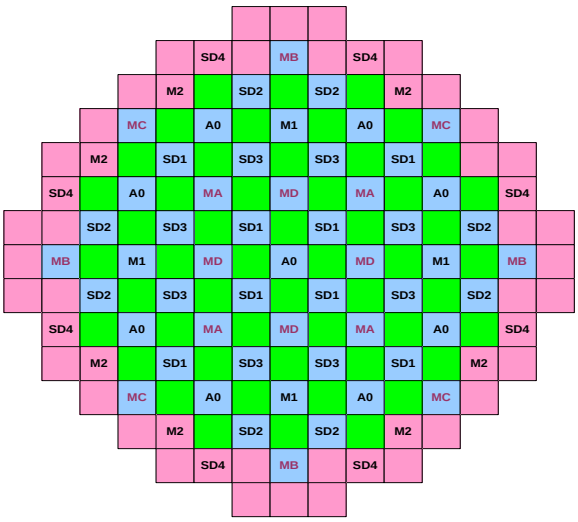

Fig. 1. PWR core configuration [11]

There is a space used to entrap gaseous fission products on the top and bottom of the fuel cladding. Each set of the fuel assembly consists of 269 (17 × 17) elements, including 264 fuel elements, 24 guide thimble elements, and one instrumentation tube. The fuel also has a total of 24 control devices on one assembly, commonly referred to as rod cluster control assemblies (RCCA) [12]. The materials used to form the control element are Ag-In-Cd, with zircaloy as the cladding. The RCCA control element device is used to regulate changes in reactivity and axial power distribution. Aside from RCCA, the PWR core contains gray rod cluster assemblies (GRCA) control components that regulate the core reactivity in response to changes in load. Light water, which is added with liquid boron which acts as a neutron absorber, is utilized as coolant and moderator. Liquid boron concentration varies in proportion to changes in reactivity caused by changes in the burn-up fraction inside the core.

Table 1. Pincel Model of PWR fuel [13]

Parameter	Cold Zero Power	Hot Full Power
Fuel Temperature (K)	300	900
Power Density (kW/kgHM)	0	38.1347
Power Density (kW/l)	0	107.284
Fuel Density (g/cm^3)	9.614	9.424
Cladding Temperature (K)	300	621.1
Cladding Density (g/cm^3)	6.550	6.550
Coolant Pressure (bar)	155.13	155.13
Coolant Temperature (K)	300	583.1
Coolant Density (g/cm^3)	1.003	0.705
Fuel Pellet Radius (mm)	4.0960	4.1274
Cladding Inner Radius (mm)	4.178	4.1896
Cladding Outer Radius (mm)	4.750	4.7609
Pin Pitch (mm)	12.6	12.626

3. METHODOLOGY

3.1 Cell Calculation

The WIMS program calculates neutron flow as a function of energy and space in a one-dimensional cell using transport theory. The DSN discrete ordinates approach was used to solve the transport equation. The fuel cell calculation step was then completed using this program package. It converts the data from the chancellor's core into a macroscopic cross-sectional constant for the reactor core material. The reactor core element was modeled as a collection of annuli made up of meat, cladding, moderator, and additional region. The WIMS program package receives input in the form of reactor fuel with different elemental compositions and temperature values. The lattices were calculated using hot zero power conditions with T_f and T_m = 600 K, as well as hot full power conditions with T_f = 900 K and T_m = 600 K [14]. The neutron spectrum in a specific geometry and groups was calculated using the software library (69 groups) in the first phase, and then utilized to summarize the amount of power into 4 groups (few groups), namely [15]:
Fast neutrons, groups 1-5 with energy range of 0.821 MeV <E ~ 10 MeV. Retarding neutrons, with energy groups 6-15 with energy range of 5,531 eV <E ~ 0.821 MeV. Resonant neutrons, group 16-45 with energy range of 0.625 eV <E ~ 5,531 eV. Thermal neutrons with energies of <0.615 eV, groups 46-69.

The atomic density of the isotope defined in the program input, as well as the microscopic cross-section of the program library, were used to calculate the macroscopic cross-section, which is needed as a coefficient in the multi-group equation. Many groups were calculated in the second section. The cell was divided into four sections, with index 1 representing the fuel meat region, index 2 representing cladding, index 3 representing moderators, and index 4 representing the additional region. Each region's dimensions and composition were determined in program inputs. The multi-group constant was divided into four groups after obtaining the multi-group spectrum in each of the four regions.

For PWR reactors with a 17 × 17 fuel device, the ThO_2-UO_2 fuel cell pin is the same. The 3 wt% U-235 fuel enrichment is designed to yield a fuel fraction of 70 GWd/t in a single cycle (3 years of full power operation = full power day). Cell pin geometry configuration with r_1 = 0.4 cm, r_2 = 0.45 cm, and r_3 = 0.677 cm fuel radius, where the outer radius is the same as a square with /2 = 0.6 cm. Table 2 and Figure 2 show the composition and configuration of the fuel cell pin geometry.

Table 2. Initial material compositions (at Hot Full Power Conditions)

Parameter	Nuclide	Weight Percent (%)	Atomic Density (1/barn cm)
Fuel	^{232}Th	65.909	1.61215E-02
	^{234}U	0.034	8.24518E-04
	^{235}U	4.291	1.03615E-03
	^{238}U	17.740	4.22957E-03
	^{16}O	12.026	4.26835E-02
Cladding	Zr-4	100	4.31438E-02
Coolant	^{1}H	11.19	4.71053E-02
	^{16}O	88.81	2.35662E-02

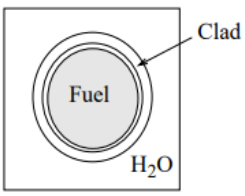

Fig. 2. The unit cell of the PWR pin [16]

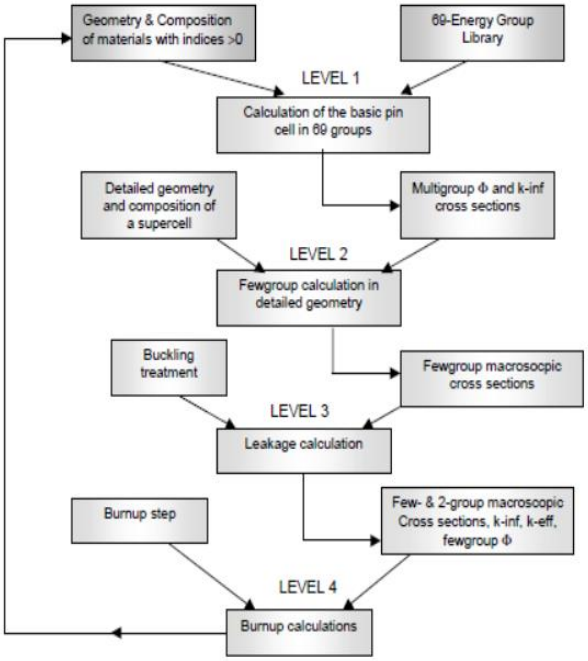

Fig. 3. Flowchart of WIMS code [17]

Because the WIMS algorithm can only calculate one-dimensional neutron transport, modeling of the core cells is required. The formation of group constants in four energy groups was calculated using cell modeling. Cell calculation using the WIMS software package and the flowchart of the WIMSD code as illustrated in Fig. 3 from the LWR cell unit consisting of fuel clusters with a square pitch arrangement. The cell unit dimensions were then determined, with each unit cell containing one fuel and a moderator. The fuel was surrounded by a moderator zone. The radius of the moderator surrounding the fuel element is then equal to the root of the aforementioned area divided by 3.14, yielding 0.53 cm. The cell dimension data was obtained from the comparable unit cell as input data for the WIMS known as the annulus, as shown in Fig. 3. Table 1 shows the atomic density that makes up the fuel pin. The goal of group constant generation is to get the average value of group constants in a cell by homogenizing it. The core buckling value (B_z^2) was acquired from the experiment as shown in Table 1 to obtain group constant values that correspond to the core conditions. The group constants for the core constituent materials were calculated under the same conditions as before. By enriching the fuel, the core k_{inf} and reaction rate were computed. Table 1 shows the pin cell shape and temperature parameters. The following steps were taken to calculate the burn-up of thorium fuel: Cells were calculated using HFP temperature conditions. On a heavy metal basis, the normal all-UO2 fuel pellets were substituted with a ThO2-UO2 combination at 94 percent of theoretical density, consisting of 75 wt% thorium and 25 wt%

uranium, with the latter enriched to 19.5 wt% U-235, for an overall enrichment of 4.8 wt% U-235 in total heavy metal. The pin cell model of a Westinghouse PWR fuel bundle unit lattice cell is shown in Figure 2. This model was used in the burnup estimates mentioned in this paper. Because all actinides in the thorium and uranium chains will be created during burn-up, this calculation is a test of all the actinide neutron libraries used by the WIMSD code and compared to MCNP, as well as a test of CASMO codes. The treatment of the group constants of each actinide was the same between calculation and reference. Tables 1 and 2 provide the pin-cell model detailed parameters for a Westinghouse PWR assembly [18]. In benchmark computations, parameters at full power were employed.

4. RESULTS AND DISCUSSION

A reference from calculation results by CASMO-4 and MIT MOCUP is shown in Table 3. The calculation results of the WIMSD-5B using existing and newest library programs are also presented in Table 3. It is obtained that the k_{inf} values of PWR pin cell using WIMSD-5B code are the same as the reference burn-up level. From WIMSD calculation, it is found that the k_{inf} value decreased with increasing fuel burnup. The values are similar to all references. The k_{inf} value at the moderator and fuel temperature of 600 K dan 900K can be burned until 72.189 MWd/kg. Compared to the result of the WIMSD-5B calculation and references, it can be said that the CASMO-4 reference is almost the same as WIMSD-5B using JEF3.1 nuclear data. MOCUP reference is almost the same as the WIMSD-5B result of calculation using ENDFB-6.8 nuclear data. The eigenvalue difference grew to around 0.032 at 60 MWd/kg, matching to estimated end-of-life core average burnup. it is because the variable and differences in that result also come from different libraries.

Table 3. Eigenvalues WIMSD-5B as a function of burn up

Burn-up (MWd/kg)	CASMO-4	MIT MOCUP	WIMS/ JEF3.1	WIMS/ ENDFB-6.8	WIMS/ ENDFB-7.0	WIMS/ ENDFB-7.1	WIMS/ ENDFB-8.0
0.000	1.23782	1.23354	1.23398	1.23381	1.24607	1.24578	1.23664
0.114	1.20071	1.19708	1.19641	1.19664	1.20823	1.20786	1.19907
5.835	1.14828	1.14466	1.14410	1.14430	1,15501	1.15579	1.14630
10.411	1.12108	1.11662	1.11812	1.11815	1.12800	1.12963	1.11944
19.563	1.07245	1.07154	1.07164	1.07164	1.07970	1.08253	1.07102
31.004	1.02014	1.02168	1.01996	1.02025	1.02593	1.02972	1.01673
40.156	0.98190	0.98453	0.982113	0.982698	0.986454	0.990771	0.976944
49.308	0.94636	0.95383	0.947483	0.948444	0.950375	0.955111	0.941717
51.596	0.93817	0.94477	0.939301	0.940354	0.941840	0.946666	0.931717
60.749	0.90701	0.91851	0.908940	0.910352	0.910225	0.915423	0.899671
72.189	0.87348	0.88449	0.876492	0.878322	0.876603	0.882305	0.865766

To evaluate the impact of various cross-section libraries in WIMSD-5B calculations, the JEF3.1, ENDF/B-VI.8, ENDF/B-VII.0, ENDF/B-VII.1, and ENDF/B-VIII.0 with their corresponding s(α,β) libraries and a mixed library of ENDF/B-VII.1 and ENDF/B-VI.8 s(α,β) were all separately used in the CASMO-4 and MOCUP calculations. All the calculations were run with the same models as references. The value of the k_{inf} from the WIMSD calculation at BOC is 1.23664 (ENDF/B-VIII.0) while CASMO-4 is 1.23782. The excess reactivity of this calculation is 19.13%, while in the reference is 19.21%. The k_{inf} value from the WIMS calculation at EOC is 0.865766 while the reference shows 0.87348. The calculation result is in good agreement with the reference when using ENDF/B-VIII.0 nuclear data.

If we compare the WIMSD calculation result to MOCUP as a reference, the k_{inf} value from the WIMSD calculation at BOC is 1.23381 (ENDF/B-VI.8), while MOCUP is 1.23354. The excess reactivity of this calculation is 18.95% and in the reference is 18.93%. The k_{inf} value from the WIMS calculation at EOC after achieving a burnup level of 72.189 MWd/kg is 0.878322, while the reference shows 0.88449. The calculation shows a good agreement with the reference when using ENDF/B-VI.8 nuclear data.

Figure 4 compares eigenvalue histories between the reference and WIMSD code. This comparison is shown at the same burnup intervals. Given that the burnup value at which reactivity approaches 0.03, which is reflective of an n-batch core-average EOC value with a 3% reactivity loss allowance for

leakage, this eigenvalue comparison shows no difference at that point. This is positive since, in order to attain equivalent accuracy in cycle length estimations, thorium-fueled cores must have better accuracy than all-uranium fueling because the slope of k_{inf} vs burnup is less steep.

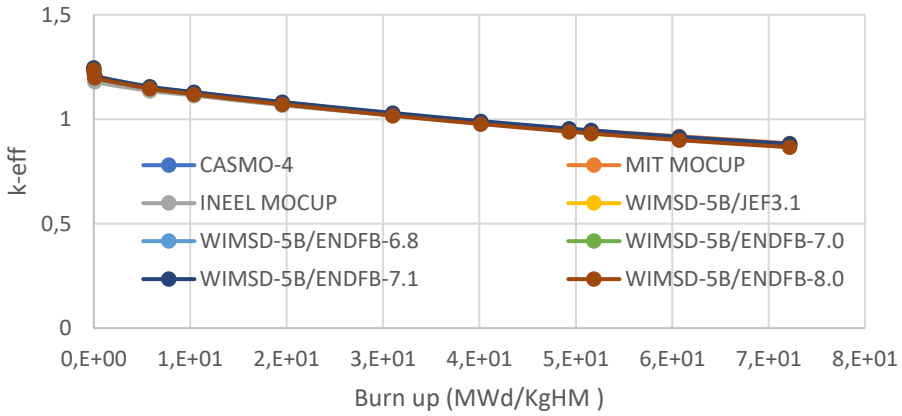

Fig. 4. Eigenvalue comparison of MOCUP, CASMO-4, and WIMSD-5B as a function of burnup

Table 4 compares isotope concentrations at 60.749 MWd/kg, which is the upper limit of discharge burn-up when using a three-batch core refueling technique. The last two columns indicate the number densities of a recent substantial ThO_2-UO_2 fuel pin cell benchmark and a uranium fuel pin cell benchmark. For a dozen or more contributions, the ThO_2 and all-U benchmark uncertainties have the widest range, but our results are single code vs code variances. Overall, our results appear to accord as well as or better than these previous recent comparisons. One interesting finding is that WIMSD-5B calculates thorium chain actinide concentrations that are almost all 4% higher than CASMO-4, whereas uranium chain actinide concentrations are on average 4% lower. According to additional calculations, in WIMSD-5B, increasing the initial Th-232 concentration by 2% while decreasing the U-238 concentration by the same amount eliminated about half of the differences. This suggests that refinement of the thorium and uranium cross-section sets (in CASMO-4, the self-shielding equivalence relation) should be investigated. WIMSD-5B had a 1% higher total end-of-cycle (EOC) heavy metal destruction, indicating that the overall average energy per fission plus capture differed somewhat between the different library codes. This is a well-known problem since few codes disaggregate the capture contribution: it is customary to adopt an 8(-1) MeV overall approximation. This means that given the same effective full power days (EFPD), WIMSD-5B will grind through more nuclide chains. Even if this nuclide has a minor effect on k_{inf}, the substantial disparity in U-234 concentrations is intriguing and deserves further investigation. Ref. [13] describes some approaches for improving macroscopic x-section accuracy, such as increasing the number of histories in MCNP. This study included two additional strategies to improve the benchmark comparison. The actinides and fission products were sorted by absorption fraction at about EOL burn-up level using ORIGEN output, and the actinides and fission products that account for the majority of absorption in fuel were classified as tracked nuclides in MOCUP. This is significant in boosting MOCUP's accuracy at high burnup, according to experience. Table 5 shows that the selected 17 actinides account for 99.9% of all actinides' neutron absorption, while Table 4 shows that the selected 41 fission products account for 97.3 percent of the absorption of fission products.

Table 4. Fractional difference between MOCUP and WIMS in isotope concentration for 60.749MWd/Kg

Isotopes	MIT MOCUP	WIMSD-5B JNDL3.2	WIMSD-5B JEF2.2	WIMSD-5B JEF3.1
Th-232	1.53469E+22	1.53805E+22	1.53700E+22	1.53530E+22
Pa-231	1.75240E+18	-	-	-
Pa-233	1.98729E+19	1.98023E+19	1.99338E+19	2.02358E+19
U-232	1.59406E+18	1.55672E+18	1.30524E+18	1.39826E+18
U-233	2.78202E+20	2.66156E+20	2.76938E+20	2.81797E+20
U-234	5.32772E+19	5.24178E+19	5.14724E+19	5.36852E+19
U-235	1.76004E+20	1.68101E+20	1.73076E+20	1.73000E+20
U-236	1.44820E+20	1.39586E+20	1.39809E+20	1.45070E+20
U-238	3.88819E+21	3.89934E+21	3.90285E+21	3.90496E+21
Np-237	1.76860E+19	1.80642E+19	1.80211E+19	1.84908E+19
Np-238	5.42397E+16	-	-	-
Np-239	7.57506E+17	7.45150E+17	7.29603E+17	7.23599E+17
Pu-238	8.88032E+18	8.71876E+18	8.90209E+18	8.69930E+18
Pu-239	5.29990E+19	4.96949E+19	5.01435E+19	5.04572E+19
Pu-240	1.79033E+19	1.80873E+19	1.79585E+19	1.80609E+19
Pu-241	1.88307E+19	1.82291E+19	1.80029E+19	1.80165E+19
Pu-242	9.93172E+18	1.03444E+19	9.76718E+18	1.01425E+19

Because CASMO employs a buckling adjustment to obtain the constants under critical conditions, while MOCUP uses the constants calculated under non-critical conditions, the variation in slope is possibly due to the difference in collapsing the one group constants for burnup contains a comprehensive discussion. Neutron cross-section libraries at room temperature were used for minor actinides and all fission products. The second method for enhancing eigenvalue comparison was to use ORIGEN to perform automatic power normalization. The MCNP flux is normalized per neutron source. We must calculate the normalization factor in terms of power level, energy per fission, and other factors in order to obtain the absolute value of flux. This can be done exogenously and roughly by averaging a number of factors, such as 202 MeV/fission for fission energy. Alternatively, because ORIGEN contains a built-in function for calculating flux from power, it can perform the aforementioned task. This work was passed to ORIGEN after a minor modification of MOCUP**.**

Table 5. Fractional Difference between CASMO and WIMS in isotope concentration for 60.749MWd/Kg

Isotopes	CASMO-4	WIMSD-5B ENDF-B6.8	WIMSD-5B ENDF-BVII.0	WIMSD-5B ENDF-BVIII.0
Th-232	1.53769E+22	1.53555E+22	1.53690E+22	1.53715E+22
Pa-231	1.70440E+18	-	-	-
Pa-233	1.95229E+19	2.01322E+19	1.99979E+19	2.00684E+19
U-232	1.56006E+18	1.48249E+18	1.43811E+18	1.43023E+18
U-233	2.74202E+20	2.82876E+20	2.72472E+20	2.70823E+20
U-234	5.15172E+19	5.25252E+19	5.34405E+19	5.34432E+19
U-235	1.78104E+20	1.74528E+20	1.68513E+20	1.62608E+20
U-236	1.39420E+20	1.46179E+20	1.46363E+20	1.48695E+20
U-238	3.88419E+21	3.90118E+21	3.90211E+21	3.90663E+21
Np-237	1.82660E+19	1.77747E+19	1.80795E+19	1.81353E+19
Np-238	5.46097E+16	-	-	-
Np-239	7.61806E+17	7.29725E+17	7.33775E+17	7.26026E+17
Pu-238	8.90932E+18	8.71580E+18	8.51888E+18	8.65050E+18
Pu-239	5.37090E+19	5.08510E+19	5.00717E+19	4.89863E+19
Pu-240	1.82233E+19	1.77920E+19	1.77774E+19	1.74175E+19
Pu-241	1.90707E+19	1.84937E+19	1.79990E+19	1.76795E+19
Pu-242	9.96772E+18	9.57290E+18	9.97119E+18	9.87572E+18

The energy released from capture reactions such as (U + n), is included in the codes as "fission energy," which is a distinction between ENDF6 and the codes. For every isotope, the maximum discrepancy between ORIGEN and CASMO is less than 5%. The difference is barely 0.25% for U-235, which accounts for the majority of fissions. The average value of 202 MeV/fission was used in the INEEL MOCUP run, which is extremely similar to the fission energy of U-235. Table 4 shows that slight discrepancies in total actinide depletion were driven by differences in fission energy employed in different codes or methodologies. It is worth noting that in this scenario, WIMS calculations for fuel temperature reactivity coefficient parameters using the new nuclear data ENDF/B-VIII.0 give consistent results to the design, whereas calculations using old nuclear data (ENDF/B-VI.8) are inconsistent or far from the design value. This is because the fission spectrum in the old nuclear data is different from the fission spectrum in the new nuclear data and the resonance handling in the physical reaction rate corresponds to the resonance of the LWR-type ThO_2 fuel. The reaction rates in the cell calculations for the isotopes U-235 and U-238 at the first group energy did not match the predictions and the effect was the rapid fission reaction of U-238 This is because the group energy mesh at the fast range is too coarse to be even more accurate. The fission equalization spectrum between U-235 and U-238 on the new nuclear data (ENDF/B-VIII.0) will produce a good cross-sectional profile resulting in parameter values that are in accordance with the design. The reaction rate of U-238 at epithermal and thermal energy yields good values against the reference. This shows that the effect of resonance on the cross-sectional generation is well calculated. It should be noted that when calculating multi-zone burn-up, such as assembly burn-up, where pin power distribution changes, it is more convenient to calculate the normalization factor in the traditional way, even though a more accurate calculation of fission energy yield is still possible using the MCNP-calculated fractional neutron loss to fission for all fissile nuclides in the modeled system.

5. CONCLUSION

WIMSD-5B code plays distinct roles in neutronic calculations. However, based on current inter-comparisons, it appears that they can agree on thorium-related computations. To compare pin cell performance to reference all-uranium lattices, it is recommended to conduct thorium usage calculations using the more user-friendly WIMSD-5B code. The average fission energy of 202 MeV/fission for thorium fuel provides findings that are comparable to more disaggregated calculations. WIMSD-5B with different nuclear data was used in additional comparisons. WIMSD-5B results are in good agreement with MOCUP and CASMO-4, notably for ENDFB-8.0, however, ENDFB-7.0 and ENDFB-7.1 deviate by more than an acceptable amount. Finding the root of these differences should help with the general issue of simulating thorium fuel. Other groups interested in thorium fuel are encouraged to provide benchmark results for the subject pin cell using other codes and cross-section sets.

ACKNOWLEDGMENT

The authors wish to thank the Head of PRTRN-BRIN and the coordinator of the BFTR Division for their kindly help and useful discussions when doing the research.

AUTHOR CONTRIBUTION

Jonny Haratua Panggabean carried out a model of pin cell input, and Santo Paulus Rajagukguk carried out cell calculation using WIMSD-5B. Both authors performed data analysis. Santo Paulus Rajagukguk and Jonny Haratua Panggabean are the main contributors of this paper. All authors read and approved the final version of the manuscript.

REFERENCES

1. Pinem S., Sembiring T.M., Surbakti T. Core Conversion Design Study of TRIGA Mark 2000 Bandung using MTR Plate Type Fuel Element. Int. J. Nucl. Energy Sci. Technol. 2018. **12**(3):222-238.
2. Surbakti T., Purwadi P. Analysis of Neutronic Safety Parameters of the Multi-Purpose Reactor–Gerrit Augustinus Siwabessy (RSG-GAS) Research Reactor at Serpong. J. Penelit. Fis. dan Apl. 2019. **9**(1):78-91.
3. Surian P., Tagor M. S., Tukiran S. Verifikasi Program PWR-fuel Dalam Manajemen Bahan Bakar PWR. JSTNI. 2015. **16**(1): 53-62.
4. Dawahra S., Khattab K., Saba G. Extending the Maximum Operation Time of the MNSR Reactor. Appl. Radiat. Isot. 2016. **115**:256-261.
5. Dawahra S., Khattab K., Saba G. Calculation and Comparison of Xenon and Samarium Reactivities of the HEU, LEU Core in the Low Power Research Reactor. Appl. Radiat. Isot. 2015. **101**:27–32.
6. Surbakti T., Pinem S., Suparlina L. Dynamic

Analysis of the Safety Criteria of the Conceptual Core Design in MTR-type Research Reactor. Atom Indonesia. 2018. **44**(2):89-97.
7. Surbakti T., Pinem S., Sembiring T.M., Hamzah A., Nabeshima K. Calculation of Control Rods Reactivity Worth of RSG-GAS First Core using Deterministic and Monte Carlo Methods. Atom Indonesia. 2019. **45**(2):69–79.
8. Pinem S., Sembiring T.M., Liem P.H. Neutronic and Thermal-hydraulic Safety Analysis for the Optimization of the Uranium Foil Target in the RSG-GAS Reactor. 2016. **42**(3):123–128.
9. Iman K., Surian P., Tagor M.S., and Tukiran S. Evaluation of Fuel Loading Pattern of PWR Core Using PWR-FUEL Code. : AIP Conference Proceedings. 2019. 2180,020007.
10. Hend S., Moustafa A., Riham R., Hesham M. Core Neutronic Characterization of Advanced Pressurized Water Reactor. Journal of Nuclear and Particle Physics. 2021. **11**(1): 7-14.
11. Zakir, M., Sarkar M., and Hossain A. Analysis of Neutronics and Thermal-Hydraulic Behavior in a Fuel Pin of Pressurized Water Reactor (PWR). World Journal of Nuclear Science and Technology. 2019. **9**: 74-83.
12. Nicholas R.B., Hans L., Arnold A., Gilad R., Michael T. Neutronic Evaluation of a PWR with Fully Ceramic Microencapsulated Fuel. Part II: Nodal Core Calculations and Preliminary Study of Thermal-Hydraulic Feedback. Annals of Nuclear Energy. 2013. **62:** 548-557.
13. Pinem S., et al. PWR Fuel Macroscopic Cross Section Analysis for Calculation Core Fuel Management Benchmark. 2019. J. Phys.: Conf. Ser. 1198 022065.
14. Surian Pinem et al. Reactivity Coefficient Calculation for AP1000 Reactor Using the NODAL3 Code. 2018. J. Phys.: Conf. Ser. 962 012057.
15. Surbakti T., Imron M. Fuel Burn-up Calculation for Working Core of the RSG-GAS Research Reactor at Batan Serpong. J. Penelit. Fis. dan Apl. 2017. 7(2):89-101.
16. Michael A.P., Sen R. S., Abderrafi M.O., Gilles Y., Brian B. Neutronic Analysis of the Burning of Transuranics in Fully Ceramic Micro-encapsulated Tri-isotropic Particle-fuel in a PWR. Nuclear Engineering and Design. 2012. **252**: 215-225.
17. Pinem S., Surbakti T., Sembiring T., et al. Optimization of Radioisotope Production at RSG-GAS Reactor using Deterministic Method. Journal Teknologi Indonesia. 2016. **1** (2):12-18.
18. Tukiran S, Surian P, Farisy Y. Calculation of PWR Thorium Pin Cell Burnup and Isotope Prediction Using WIMSD-5B Code. Journal of Physics: Conference Series 1811. 2021. 012047